

## Anisotropy of the Raman Spectra of Nanographite Ribbons

L. G. Cançado,<sup>1</sup> M. A. Pimenta,<sup>1</sup> B. R. A. Neves,<sup>1</sup> G. Medeiros-Ribeiro,<sup>2</sup> Toshiaki Enoki,<sup>3</sup> Yousuke Kobayashi,<sup>3</sup> Kazuyuki Takai,<sup>3</sup> Ken-ichi Fukui,<sup>3</sup> M. S. Dresselhaus,<sup>4,5</sup> R. Saito,<sup>6</sup> and A. Jorio<sup>1</sup>

<sup>1</sup>*Departamento de Física, Universidade Federal de Minas Gerais, Belo Horizonte, Brazil*

<sup>2</sup>*Laboratório Nacional de Luz Síncrotron, Campinas, Brazil*

<sup>3</sup>*Department of Chemistry, Tokyo Institute of Technology, 2-12-1, Ookayama, Meguro-ku, Tokyo 152-8551, Japan*

<sup>4</sup>*Department of Physics, Massachusetts Institute of Technology, Cambridge, Massachusetts 02139-4307, USA*

<sup>5</sup>*Department of Electrical Engineering and Computer Science, Massachusetts Institute of Technology, Cambridge, Massachusetts 02139-4307, USA*

<sup>6</sup>*Department of Physics, Tohoku University and CREST JST, Aoba Sendai 980-8578, Japan*

(Received 16 January 2004; published 23 July 2004)

A polarized Raman study of nanographite ribbons on a highly oriented pyrolytic graphite substrate is reported. The Raman peak of the nanographite ribbons exhibits an intensity dependence on the light polarization direction relative to the nanographite ribbon axis. This result is due to the quantum confinement of the electrons in the 1D band structure of the nanographite ribbons, combined with the anisotropy of the light absorption in 2D graphite, in agreement with theoretical predictions.

DOI: 10.1103/PhysRevLett.93.047403

PACS numbers: 78.30.Na, 73.22.-f, 78.66.Tr, 78.67.Ch

Graphite-related materials have been the object of many studies [1] in the last decades including, and, in particular, carbon nanotubes that can be obtained by rolling up a graphene sheet into a tube of nanometric diameter [2]. This large interest in carbon nanotubes is owing to the fact that they are quasi-one-dimensional (1D) systems and have many properties related to quantum confinement [2]. Another form of a 1D carbon system is a strip of a graphene sheet, which is called a nanographite ribbon in the literature [3,4]. Previous works have shown the existence of 1D graphite nanostructures in polyperinaphthalene [5,6] and in fibers obtained from carbon nanotubes subjected to high temperature and pressure [7]. The synthesis of nanographite ribbons grown from a SiC arc discharge has been reported, including the observation of a ribbon bifurcated along the *c* axis, forming a nano-Y junction [8]. This is a promising structure in the field of nanoelectronic devices because of its interesting transport properties [9].

In this paper, we present a polarized Raman study of a nanographite ribbon deposited on a highly oriented pyrolytic graphite (HOPG) substrate. The Raman peaks of the nanographite ribbon and the HOPG are split due to different thermal expansions of the ribbon and the substrate. The Raman signal from a nanographite ribbon is as intense as that of the HOPG substrate and has a strong dependence on the light polarization. In order to explain these results, we present a model that takes into account the quantum confinement of the electrons in the 1D structure of nanographite ribbons and the anisotropy in the light absorption in 2D graphite. The Raman results shown here confirm the presence of nodes in the optical absorption spectra of graphite, in agreement with theoretical predictions [10].

The sample used in the experiment was prepared by the electrophoretic deposition of diamond nanoparticles on a

HOPG substrate [11]. At a heat-treatment temperature of 1600 °C, the diamond nanoparticles are graphitized, forming nanographite sheets [12]. Atomic force microscopy (AFM) images of the sample were acquired using a Nanoscope IV MultiMode microscope from Veeco Instruments, operating in the intermittent contact (tapping) mode, at room temperature, using standard Si cantilevers. Figure 1(a) shows an AFM image, where many ribbons parallel to each other are observed. The average width of the ribbons is 8 nm and the length can be as large as 1 μm. Figure 1(b) shows an AFM image where the presence of a ribbon near a step of the HOPG substrate is evident. The ribbon is larger than 500 nm in length. The

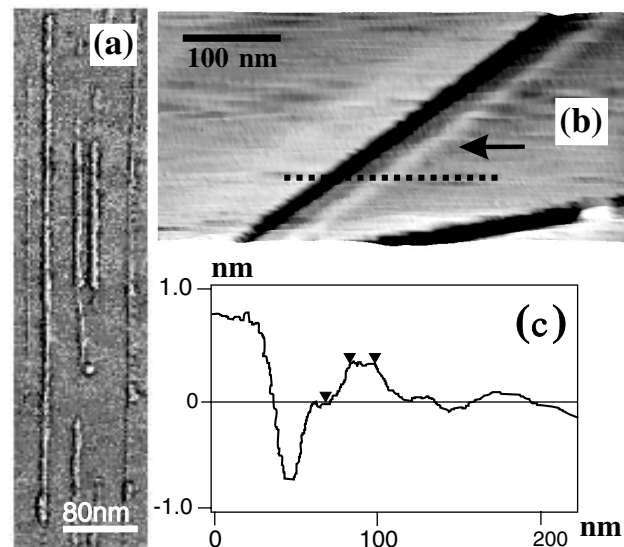


FIG. 1. (a) AFM image of many ribbons parallel to each other. (b) AFM image of a nanographite ribbon near a step. The arrow indicates the position of the ribbon for reference. (c) The height profile obtained through the dotted line in (b).

height profile [Fig. 1(c)] shows a height of 0.35 nm, which corresponds exactly to the interlayer distance of bulk graphite, indicating that the ribbon has only one layer of atoms.

Backscattering micro Raman spectra were taken at room temperature using a DILOR XY triple monochromator. The laser energy, spot area, and power density on the sample were 2.41 eV,  $10^{-8}$  cm<sup>2</sup>, and  $3 \times 10^5$  W/cm<sup>2</sup>, respectively. A half-wave plate was coupled to the microscope in order to rotate the polarization of the incident and the scattered light, allowing measurements to be made of the angular dependence of the polarized Raman spectra. The spectra were taken in the region of the sample where the ribbons depicted in Fig. 1(a) were observed. By scanning the sample, the Raman signal from a particular nanographite ribbon is obtained when the light spot reaches a ribbon that is in resonance with  $E_{\text{laser}} = 2.41$  eV.

Figure 2(a) shows the Raman spectra obtained with different polarization directions for the incident light. The propagation of the incident light is perpendicular to the graphite plane and  $\theta$  is the angle between the longitudinal direction of the ribbon and the light polarization ( $\vec{P}$ ) [inset to Fig. 2(a)]. The information about the ribbon direction was obtained by AFM [Fig. 1(a)]. Note that the Raman band is composed of two peaks, centered at 1568 and 1579 cm<sup>-1</sup>, and these will be called the  $G_1$  and  $G_2$

peaks, respectively. By increasing the angle  $\theta$ , the intensity of the  $G_1$  peak decreases gradually, while the intensity of the  $G_2$  peak remains constant. Figure 2(b) shows the angular dependence of the  $G_1$  peak intensity fitted by a  $\cos^2\theta$  curve. Figure 2(c) shows the dependence of the  $G_1$  and  $G_2$  peak frequencies on the laser power used in the experiment, as discussed below.

The angular dependence of the Raman spectra shown in Figs. 2(a) and 2(b) can be explained by considering the selection rules for light absorption in graphite and the quantum confinement in a 1D nanographite ribbon. The Raman efficiency is related to the absorption coefficient since the Raman scattering is a third order process which involves the absorption of an incident photon, the creation (or annihilation) of a phonon, and the emission of a scattered photon. According to theoretical calculations for 2D graphite, the probability of light absorption  $W(\vec{k})$  per unit time is associated with the polarization vector of incident light  $\vec{P} = (p_x, p_y)$  and with the wave vector  $\vec{k} = (k_x, k_y)$  of the electron by [10]

$$W(\vec{k}) \propto \frac{|\vec{P} \times \vec{k}|^2}{k^2}, \quad (1)$$

where  $\vec{k}$  is measured from the  $K$  point situated at the corner of the first Brillouin zone. For points  $k$  near the  $K$  point, the energy dispersion of  $\pi$  electrons is symmetric around  $K$  and is linearly proportional to  $k$ , that is,

$$E(k) = \pm \frac{\sqrt{3}\gamma_0 a}{2} k, \quad (2)$$

where  $\gamma_0$  is the tight binding overlap integral parameter and  $a = 0.246$  nm is the graphite in-plane lattice parameter [2]. In the light absorption process with a fixed laser energy ( $E_{\text{laser}}$ ), the energy separation between valence and conduction bands is  $E_{\text{laser}} = 2|E(k)|$ . Therefore, the wave vector of electrons involved in the light absorption process forms a circle around the  $K$  point with radius  $k_{\text{abs}} = E_{\text{laser}}/\sqrt{3}\gamma_0 a$ . We are disregarding here the trigonal warping effect [2], considering that optical transitions occur sufficiently near to the  $K$  point.

Equation (1) shows that the light absorption has a maximum for electrons with a  $\vec{k}$  vector perpendicular to the polarization of the incident light ( $\vec{P}$ ) and is zero for electrons with  $\vec{k}$  parallel to  $\vec{P}$ . This fact is not measurable in 2D crystalline graphite because the density of electrons involved in the absorption process is isotropic in the graphene plane, and no changes in the Raman intensity can be observed by rotating the incident light polarization [10]. Therefore, based on the fact that the observed  $G_2$  peak frequency is not affected in the angular dependence depicted in Fig. 2(a), it can be concluded that  $G_2$  is associated with the  $E_{2g}$  vibrational mode of the HOPG substrate [13].

The situation is different for nanographite ribbons because, in this case, the  $k$  dependence for the light

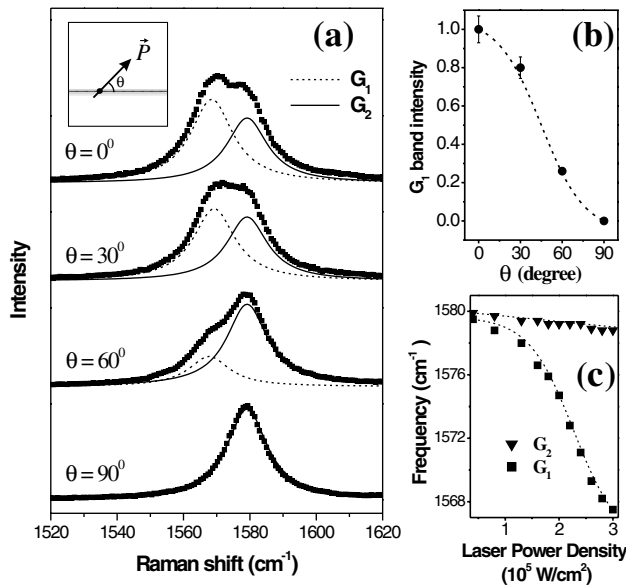


FIG. 2. (a) Raman spectra obtained for light incident with different polarization angles ( $\theta$ ) with respect to the ribbon direction. The inset shows a schematic figure of the sample (horizontal gray line) showing the direction between the ribbon axis and the light polarization vector ( $\vec{P}$ ). (b) Intensity of the  $G_1$  peak versus  $\theta$ . The dotted line is a  $\cos^2\theta$  theoretical curve. The error bars are associated with baseline corrections. (c) Raman frequencies of the  $G_2$  (triangles) and  $G_1$  (squares) peaks as a function of the laser power density.

absorption process is important. Figure 3(a) shows the network of a zigzag nanographite ribbon with  $N = 8$ , where  $N$  is the number of dimer lines. The unit cell has  $2N$  atoms and is defined by the longitudinal ( $\vec{L}$ ) and transverse ( $\vec{T}$ ) vectors. The Brillouin zone, depicted in Fig. 3(b), is formed by  $N$  lines (the so-called cutting lines) parallel to the direction of the  $\vec{K}_L$  vector [3,4]. The wave vectors are continuous along the direction of  $\vec{K}_L$  for a ribbon of infinite length. On the other hand, because of the finite size of the nanographite ribbon in the transverse direction, there are  $N$  possible discrete  $k$  values separated by  $|\vec{K}_T|$ . The electronic structure of nanographite ribbons is formed by 1D subbands due to the quantization of the  $k$  space in the transverse ribbon direction. These 1D subbands are obtained by folding the dispersion curves of 2D graphite along cutting lines [3,4]. Therefore, the electronic density of states (DOS) exhibits van Hove singularities [3,4,14–16].

The optical absorption process in nanographite ribbons is associated with electronic transitions between the valence ( $\pi$ ) and conduction ( $\pi^*$ ) 1D subbands [17,18]. The quantum confinement of the electrons in a 1D structure restricts the wave vectors ( $\vec{k}$ ) of the electrons involved in the absorption process that are associated with transitions between van Hove singularities in the valence and conduction bands. The optical transition energies between

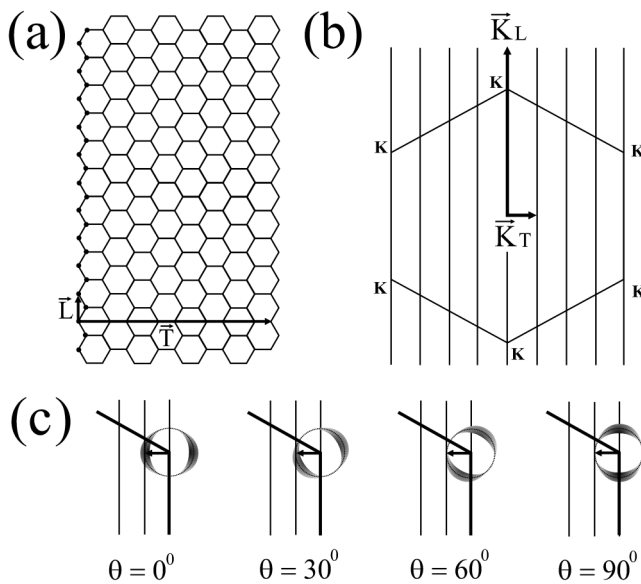


FIG. 3. (a) A zigzag nanographite ribbon network with  $N = 8$ .  $\vec{L}$  and  $\vec{T}$  are the longitudinal and transverse vectors that define the unit cell. (b) The reciprocal lattice of zigzag nanographite ribbon shown in (a).  $\vec{K}_L$  and  $\vec{K}_T$  represent reciprocal lattice vectors. (c) The  $k$  dependence for the probability of absorption  $[W(\vec{k})]$  near to a  $K$  point, for the four different values of  $\theta$ . The dark region gives a large absorption coefficient. The arrows indicate the  $\vec{K}_T$  vectors that coincide with a maximum in the optical absorption for  $\theta = 0^\circ$  and with a node in the optical absorption for  $\theta = 90^\circ$  [10].

van Hove singularities are different for nanographite ribbons with different widths or crystalline directions of the  $\vec{L}$  vector [Fig. 3(a)]. By scanning the sample, the Raman signal from a particular nanographite ribbon is obtained when the light spot reaches a ribbon that is in resonance with  $E_{\text{laser}} = 2.41$  eV. Note that the number of C atoms from the HOPG substrate under the laser spot is at least 100 times larger than the number of C atoms from the ribbon. The observation of the Raman signal from a nanographite ribbon with an intensity similar to the Raman signal from the HOPG substrate is possible by considering the quantum confinement of the electronic states in the ribbon.

A van Hove singularity in the electronic DOS occurs when a cutting line is tangential to the circle of radius  $k_{\text{abs}}$ . This condition is obtained for electrons with a wave vector along the  $\vec{K}_T$  direction. When the photon energy of the incident laser is resonant with an allowed transition between singularities in the 1D density of electronic states, the Raman scattering cross section diverges, and the intensity of the Raman peak is enhanced. This resonant mechanism selects the  $k$  vector of electrons and only those along the  $\vec{K}_T$  direction are involved in the absorption process, that is,  $\vec{k} \parallel \vec{K}_T$ .

According to Eq. (1), the light absorption probability is proportional to the square of the projection of the polarization vector ( $\vec{P}$ ) in the direction perpendicular to the vector  $\vec{K}_T$ , that is the longitudinal ribbon direction. Figure 3(c) shows that the vector  $\vec{K}_T$  coincides with a maximum in the optical absorption for  $\theta = 0^\circ$  and with a node in the optical absorption for  $\theta = 90^\circ$ . As  $\theta$  is the angle between  $\vec{P}$  and the longitudinal ribbon direction, we expect that  $W(\vec{k}) \propto \cos^2\theta$ . Since the Raman intensity is proportional to the number of absorbed photons, it must be also proportional to  $\cos^2\theta$ . As shown in Figs. 2(a) and 2(b), the intensity of the  $G_1$  peak has a maximum value for the incident light polarized parallel to the longitudinal ribbon direction ( $\theta = 0^\circ$ ), decreases according to  $\cos^2\theta$ , and is null when  $\vec{P}$  is perpendicular to the longitudinal ribbon direction ( $\theta = 90^\circ$ ). The experimental results shown in Figs. 2(a) and 2(b) are in excellent agreement with theoretical predictions and allow us to conclude that the  $G_1$  peak is indeed associated with the  $E_{2g}$  vibrational mode of the nanographite ribbon. It is important to emphasize that the analysis above is valid not only for zigzag-type ribbons, but also for ribbons with any type of edge form.

Finally, it is worth analyzing the frequency shift of the two peaks,  $G_1$  and  $G_2$  depicted on Fig. 2(c). In fact, this shift is due to a thermal effect. Using a low laser power density, one just observes a single peak for the  $G$  band at  $1580 \text{ cm}^{-1}$ . The  $G$  band splits into two peaks when the laser power is increased. The frequencies of these two peaks decrease with increasing laser power, owing to the increase in the local temperature. However, the  $G_1$  frequency decreases nonlinearly, whereas the  $G_2$  frequency

exhibits only a small laser power dependence. This is expected, since the Raman frequency of nanosized graphite systems exhibits a stronger thermal dependence compared to bulk graphite [19–21]. The high thermal conduction coefficient in the graphene plane avoids the excessive heating with the increase of the laser power density, keeping the lattice parameters almost constant. However, in finite size systems, the heat dissipation is less efficient, and therefore the force constants are more affected, providing a strong dependence of the Raman frequency on laser power density, as shown in Fig. 2(c). It is interesting to emphasize that this thermal effect makes possible the observation of a Raman signal from a nanographite ribbon sitting on a graphite bulk substrate.

In summary, this Letter presents a polarized Raman study of nanographite ribbons which shows evidence for the anisotropic character of light scattering in this system. The results give experimental evidence for the predicted existence of a node in the optical absorption in graphite and the presence of van Hove singularities in the DOS of the nanographite ribbons. A more complete characterization of the DOS profile could be performed using a tunable laser. This is a challenging experiment that requires a tunable laser system with high laser power to separate the Raman signal from nanographite ribbons and the HOPG substrate.

This work is supported by the Instituto de Nanociências and FAPEMIG, Brazil. L. G. C. acknowledges support from the Brazilian Agencies CAPES and CNPq, and LNLS for his visit. M. A. P. acknowledges UEC for supporting his visit. A. J. acknowledges support from PRPq-UFGM and Profix-CNPq, Brazil. T. E., Y. K., K. T., and K. F. acknowledge a Grant in Aid for Research for the Future Program, Nanocarbons, and a Grant in Aid for Research (No. 15105005) from JSPS. R. S. acknowledges a Grant in Aid (No. 13440091) from the Ministry of Education, Japan.

---

[1] M. S. Dresselhaus, G. Dresselhaus, K. Sugihara, I. L. Spain, and H. A. Goldberg, *Graphite Fibers and Filaments*, Springer Series in Material Science Vol. 5 (Springer-Verlag, Berlin, 1988).

- [2] R. Saito, G. Dresselhaus, and M. S. Dresselhaus, *Physical Properties of Carbon Nanotubes* (Imperial College Press, London, 1998).
- [3] M. Fujita, K. Wakabayashi, K. Nakada, and K. Kusakabe, *J. Phys. Soc. Jpn.* **65**, 1920 (1996).
- [4] K. Nakada, M. Fujita, G. Dresselhaus, and M. Dresselhaus, *Phys. Rev. B* **54**, 17 954 (1996).
- [5] Mutsuaki Murakami, Sumio Iijima, and Susumu Yoshimura, *J. Appl. Phys.* **60**, 3856 (1986).
- [6] M. Yudasaka, Y. Tasaka, M. Tanaka, H. Kamo, Y. Ohki, S. Usami, and S. Yoshimura, *Appl. Phys. Lett.* **64**, 3237 (1994).
- [7] M. Zhang, D. H. Wu, C. L. Xu, Y. F. Xu, and W. K. Wang, *Nanostruct. Mater.* **10**, 1145 (1998).
- [8] Yubao Li, Sishen Xie, Weiya Zhou, Dongsheng Tang, Xiao-Ping Zou, Zhuqin Liu, and Gang Wang, *Carbon* **39**, 626 (2000).
- [9] K. Wakabayashi, *Phys. Rev. B* **64**, 125428 (2001).
- [10] A. Gruneis, R. Saito, Ge. G. Samsomidze, T. Kimura, M. A. Pimenta, A. Jorio, A. G. Souza Filho, G. Dresselhaus, and M. S. Dresselhaus, *Phys. Rev. B* **67**, 165402 (2003).
- [11] A. M. Affoune, B. L. V. Prasad, Hirohiko Sato, and Toshiaki Enoki, *Langmuir* **17**, 547 (2001).
- [12] A. M. Affoune, B. L. V. Prasad, Hirohiko Sato, Toshiaki Enoki, Yutaka Kaburagi, and Yoshihiro Hishiyama, *Chem. Phys. Lett.* **348**, 17 (2001).
- [13] F. Tuinstra and J. L. Koenig, *J. Chem. Phys.* **53**, 1126 (1970).
- [14] K. Wakabayashi, M. Fujita, H. Ajiki, and M. Sigrüst, *Phys. Rev. B* **59**, 8271 (1999).
- [15] Y. Miyamoto, K. Nakada, and M. Fujita, *Phys. Rev. B* **59**, 9858 (1999).
- [16] F. L. Shyu, M. F. Lin, C. P. Chang, R. B. Chen, J. S. Shyu, Y. C. Wang, and C. H. Liao, *J. Phys. Soc. Jpn.* **70**, 3348 (2001).
- [17] M. F. Lin and F. L. Shyu, *J. Phys. Soc. Jpn.* **69**, 3529 (2000).
- [18] C. W. Chiu, F. L. Shyu, C. P. Chang, R. B. Chen, and M. F. Lin, *J. Phys. Soc. Jpn.* **72**, 170 (2003).
- [19] Ping-Heng Tan, Yuan-Ming Deng, Qian Zhao, and Wen-Chao Cheng, *Appl. Phys. Lett.* **74**, 1818 (1999).
- [20] H. Herchen and M. A. Cappelli, *Phys. Rev. B* **43**, 11 740 (1991).
- [21] E. S. Zouboulis and M. Grimsditch, *Phys. Rev. B* **43**, 12 490 (1991).